THE JOURNAL OF BIOLOGICAL CHEMISTRY
Vol. 276, No. 45, Issue of November 9, pp. 42122–42130, 2001
Printed in U.S.A.


# Distinct Binding Specificity of the Multiple PDZ Domains of INADL, a Human Protein with Homology to INAD from *Drosophila melanogaster**

Received for publication, May 9, 2001, and in revised form, August 6, 2001
Published, JBC Papers in Press, August 16, 2001, DOI 10.1074/jbc.M104208200

**Paola Vaccaro‡§, Barbara Brannetti‡, Luisa Montecchi-Palazzi‡, Stephan Philipp¶, Manuela Helmer Citterich‡, Gianni Cesareni‡, and Luciana Dente‡‖****

*From the ‡Department of Biology Enrico Calef, University of Rome Tor Vergata, Via della Ricerca Scientifica, 00133 Rome, Italy, ‖Department of Physiology and Biochemistry, University of Pisa, Via Carducci, 56010 Pisa, Italy, and ¶Institute of Pharmakologie und Toxikologie, University of Saarlandes, D66421 Homburg, Germany*

**PDZ domains are protein-protein interaction modules that typically bind to short peptide sequences at the carboxyl terminus of target proteins. Proteins containing multiple PDZ domains often bind to different transmembrane and intracellular proteins, playing a central role as organizers of multimeric complexes. To characterize the rules underlying the binding specificity of different PDZ domains, we have assembled a novel repertoire of random peptides that are displayed at high density at the carboxyl terminus of the capsid D protein of bacteriophage λ. We have exploited this combinatorial library to determine the peptide binding preference of the seven PDZ domains of human INADL, a multi-PDZ protein that is homologous to the INAD protein of *Drosophila melanogaster*. This approach has permitted the determination of the consensus ligand for each PDZ domain and the assignment to class I, class II, and to a new specificity class, class IV, characterized by the presence of an acidic residue at the carboxyl-terminal position. Homology modeling and site-directed mutagenesis experiments confirmed the involvement of specific residues at contact positions in determining the domain binding preference. However, these experiments failed to reveal simple rules that would permit the association of the chemical characteristics of any given residue in the peptide binding pocket to the preference for specific amino acid sequences in the ligand peptide. Rather, they suggested that to infer the binding preference of any PDZ domain, it is necessary to simultaneously take into account all contact positions by using computational procedures. For this purpose we extended the SPOT algorithm, originally developed for SH3 domains, to evaluate the probability that any peptide would bind to any given PDZ domain.**

A large number of interactions in the cell are mediated by families of protein binding modules that are found repeatedly and in different combinations in several proteins. Typically these modules mediate protein-protein interactions through recognition of short peptides in the target protein (1). Several approaches, based upon the screening of repertoires of combinatorial peptides, have been developed to investigate the recognition specificity of these domain families. Phage display of small peptides of random sequence has been successfully used for the characterization of binding domains such as SH2, SH3, WW, EH, etc. (reviewed in Ref. 2). PDZ domains (identified as conserved elements in postsynaptic density protein PSD-95, Disc-large tumor suppressor Dlg, Zonula occludens protein ZO-1) differ from the remaining domains since they bind to specific carboxyl-terminal sequences of target proteins and/or dimerize with other PDZ domains (reviewed in Ref. 3). This peculiarity has limited the possibility of using "classical" peptide repertoires displayed by fusion to M13 coat proteins, since these display systems present random peptides by fusing them to the amino terminus of pIII or pVIII coat proteins. As a consequence, PDZ specificity has been studied using repertoires of chemically synthesized random peptides (4, 5) or alternative display systems, such as fusion to the carboxyl terminus of Lac repressor (6). Cyclic peptides may also be forced into conformations that mimic carboxyl termini (7). More recently Fuh *et al.* (8) show that the M13 pVIII protein can tolerate peptide extensions at its carboxyl terminus and have assembled and exploited a repertoire of random carboxyl-terminal peptides to study the binding specificity of two PDZ domains of the protein MAGI (membrane-associated guanylate kinase with inverted orientation). This approach yielded a family of specific ligands for PDZ-2, whereas only one ligand for the other domain (PDZ-3) could be identified. This result is probably a consequence of the low copy number of the displayed recombinant peptides, because even when the display vector was modified to increase the display density by 10-fold, the majority of the phage coat was made up of wild type pVIII molecules supplied by the helper phage (8, 9). Furthermore, because of the topology of the assembled pVIII coat protein, whose carboxyl terminus is buried into the capsid in contact with the genomic single-stranded DNA (10), it is possible that only a fraction of peptides of random sequence can be tolerated in this display system without causing steric hindrance.

To overcome these limitations we have designed a new type of combinatorial library, where random peptides are displayed on the surface of λ phage by fusion to the carboxyl terminus of the D-capsid protein. In this system about 95% of the D proteins are recombinant, and because the carboxyl terminus of

* This work was supported by grants from the Associazione Italiana Ricerca sul Cancro, Cofinanziamento Ministero dell'Università e della Ricerca Scientifica e Tecnologica (MURST Cofin), and Consiglio Nazionale delle Ricerche target project Biotechnology (to G. C.) and MURST Cofin (to L. D.). The costs of publication of this article were defrayed in part by the payment of page charges. This article must therefore be hereby marked "*advertisement*" in accordance with 18 U.S.C. Section 1734 solely to indicate this fact.

§ Present address: Kenton laboratories, c/o Sigma-Tau, via Pontina Km 30.400, 00040, Pomezia, Rome, Italy.

** To whom correspondence should be addressed: Dept. of Physiology and Biochemistry, University of Pisa, via G. Carducci 13, 56010 Pisa, Italy. Tel.: 39-050-878-356; Fax: 39-050-878486; E-mail: dentel@dfb.unipi.it.

this protein does not appear to be involved in head formation (11), subunits containing short peptide extensions are expected to be assembled at the same high density irrespective of their sequence.

To investigate the binding specificity of different PDZ domains, we have panned such a carboxyl-terminal library with each of the PDZ modules of hINADL,[1] a protein homologous to dINAD of *Drosophila melanogaster* belonging to the family of multi-PDZ proteins (12). dINAD is the prototypical member of this family characterized by the exclusive presence of multiple copies of PDZ domains without any catalytic or other known binding domain (13). The five PDZ domains of dINAD participate in distinct structural and signaling functions by binding to different protein partners to assemble a macromolecular transduction complex that enables high speed signaling in *Drosophila* photoreceptors (3).

The hINADL gene was isolated because of its sequence homology to dINAD and was found to be expressed in different spliced forms in various organs and tissues (12). Differently from dINAD, hINADL encodes a protein that contains seven PDZ domains. Although no natural partner has been characterized to date, the identification of PDZ domains repeated in tandem suggests that hINADL also functions as a molecular scaffold for organizing protein complexes. In this manuscript we analyze the binding specificity of each of the seven PDZ domains of hINADL, and we implement a computational procedure to infer the binding probability of different peptide-domain complexes.

## EXPERIMENTAL PROCEDURES

*Materials*—Bacterial strains used were *Escherichia coli* BL21(DE3), hsdS gal (λc*I*ts857 *ind*1 *S*am7 *nin*5 *lac*UV5-T7 gene 1) and BB4, *supF*58 *supE*44 *hsdR*514 *galK*2 *galT*22 *trpR*55 *metB*1 *tonA* Δ*lac*U169 F′ [*proAB*$^+$ *lacI*$^q$ *lacZ*ΔM15 Tn*10* (*tet*$^r$)]. Bovine serum albumin and Tween 20 were from Sigma. pGEX-2TK, glutathione-Sepharose, and anti-glutathione *S*-transferase (GST) antibody were from Amersham Pharmacia Biotech. *Spe*I and *Not*I restriction enzymes and T4 ligase were from Biolabs. Dynabeads were from DYNAL; Gigapack® III Gold packaging extract was from Stratagene.

*Library Construction*—The λ display vector, λDsplay1, is described in detail in Castagnoli *et al.* (14). It contains an additional D gene under the control of $p_{TRC}$ promoter followed by *Spe*I and *Not*I unique cloning sites. To assemble the carboxyl-terminal peptide library, the oligonucleotide R384 (5′-GTCGAATTCTTAGCGGCCGCATTA-3′) was used as a primer for oligonucleotide R383 (5′-TCATGCCATGGAGACTAGT-(**NNK**)$_9$**TAA**TGCGGCCGCTAAGAATTCGAC-3′) (where K = G or T) containing nine degenerate codons followed by the stop codon TAA (in bold). The restriction sites *Spe*I and *Not*I are underlined. The two oligonucleotides were biotinylated at their 5′ end and annealed by mixing 200 pmols of each in 200 μl, heating at 65 °C for 5′, and slowly cooling to room temperature. The annealed DNA was made double-stranded by incubating for 2 h at 37 °C after the addition of dNTPs (500 μM) and 50 units of the Klenow fragment of DNA polymerase I. After digestion with *Spe*I and *Not*I, the biotinylated terminal fragments were removed using streptavidin-Dynabeads. The *Spe*I/*Not*I DNA fragments were passed through a Sephadex G-50 column, ligated into *Spe*I/*Not*I-digested λ vector, and incorporated into phage particles by *in vitro* packaging. Bacteriophages were propagated in BB4 cells on L agar plates.

*GST Fusion Proteins*—cDNA sequences coding for the seven INADL PDZ domains (accession number AJ224747) were amplified by polymerase chain reaction from plasmid hINADL, kindly provided by S. Philipp and V. Flockerzi (12), using oligonucleotides designed to hybridize to the DNA regions flanking the PDZ domains coding sequences. The borders of the domains are indicated in Fig. 1. The amplified fragments were inserted in-frame into pGEX-2TK (Amersham Pharmacia Biotech) using the *Bam*HI and *Eco*RI restriction sites. GST fusion proteins were expressed in *E. coli* BL21(DE3) and purified according to manufacturer's instructions.

*Panning*—Affinity selection of the peptide displaying λ phages was performed as described in Zucconi *et al.* (15) with minor modifications. Glutathione-Sepharose 4B beads (30 μl of slurry) were coated with ~10 μg of GST fusion proteins and pre-incubated in phosphate-buffered saline with 3% bovine serum albumin for 4 h at 4 °C. The library was then added (about $2 \times 10^9$ plaque-forming units), and the incubation was performed for 1 h at 4 °C in SM buffer (150 mM NaCl, 10 mM $MgSO_4$, 50 mM Tris HCl, pH 7.5). The Sepharose beads were then collected by centrifugation and washed 10 times with ice-cold phosphate-buffered saline, Tween 0.05%. The adsorbed (A) and non-adsorbed (N) phages were titered by counting plaques on a BB4 bacterial lawn. The adsorbed phages were propagated by plate lysate, eluted, concentrated by polyethylene glycol precipitation, and subjected to the next panning cycle. After three selection cycles, phage clones were purified and tested by solid phase immunoassay against their bait proteins.

*Solid Phase Immunoassay, Phage Enzyme-linked Immunosorbent Assay*—Microtiter wells were coated overnight at 4 °C with anti-GST antibody (10 μg/ml), and after washing, PDZ-GST fusion proteins (or control GST) were added at a concentration of 20 μg/ml phosphate-buffered saline. After washing, about $10^7$ phage particles of each selected clone were added to the appropriate well and incubated overnight at 4 °C. The bound phage particles were revealed using a purified IgG fraction of anti-λ serum (rabbit) diluted 1:500 from a170 μg/ml stock (16) and a secondary, alkaline phosphatase-conjugated, anti-rabbit goat antibody (Sigma A-8025). The chromogenic reaction was developed for 1 h at 37 °C by adding *p*-nitrophenyl phosphate substrate (Sigma 1047), and the reading was performed at 405–620-nm dual wavelength.

*Sequencing*—The DNA inserts of selected phage clones were amplified by polymerase chain reaction, purified on QIAquick columns (Qiagen), and sequenced using an ABI Prism™ 310 genetic analyzer (PerkinElmer Life Sciences).

*Mutagenesis*—Site-specific mutagenesis was performed using the unique site mutagenesis kit (Amersham Pharmacia Biotech) that utilizes a two-primer system to generate site-specific mutations in double-stranded plasmids. PGEX-PDZ7 was used as a template. The mutagenic oligonucleotides were R722, 5′-CCTTCTTCATAGACTGAACGG-ATAACTATAGCATTC-3′ (for PDZ7RS), and R723, 5′-GGCTGTGATG-GCTTCTGCCAGGCTGGAGTTCCTCAG-3′ (for PDZ7LA).

*Homology Modeling*—The model structures of the PDZ7 wild type, LA, and RS mutant domains of hINADL were built using the PSD-95-3 PDZ domain (Protein Data Bank code: 1be9) as template structure (17). Direct alignment of the two sequences gives an overall similarity of 61 and 47% identity. Modeling was carried out on a Silicon Graphics $O_2$ work station using the program InsightII (18). The model was subjected to limited energy refinement (program Discover, steepest descent algorithm, Molecular Simulations S.a.r.l.). The SearchLoop Protein command was used to find suitable geometries for residue insertion in one loop of the defined model. The SURFNET procedure (19) was used to measure the volumes of the cavities with minimum and maximum gap sphere radii equal to 1 and 4 Å, respectively.

*Computational Analysis*—Details about the SPOT procedure were essentially as previously described (20). The contact matrix shown in Fig. 3 was derived from the analysis of the three-dimensional structures of PDZ domain-ligand complexes solved by x-ray crystallography, Protein Data Bank entry codes 1qav (syntrophin-nNOS) (21), 1kwa (Cask-LIN-2) (22), 1be9 (PSD95-3) (23). The residue-residue interaction data base was constructed starting from a total of 311 peptides selected from 10 different PDZ domains: 90 ligands of nNOS (6, 24); 8 of Af6 (25, 26); 8 of PSD95-2 (27, 28); 13 of PSD95-3 (6, 29)[2]; 6 of α1-syntrophin (6, 7, 21, 30); 5 of Cask (31, 32); 24 of dINAD1 (33, 34); 33 of $Na^+/H^+$ exchanger regulatory factor (NHERF)-1 and 16 of NHERF-2 (35); 10 of MAGI-2 (8); plus 97 ligands of the 7 PDZ domains of INADL described in this paper (Fig. 1). The frequency of the residues in the contacting positions was deduced from the alignment of the carboxyl-terminal portions of the ligand peptides of each PDZ domain.

## RESULTS

*Construction of a Carboxyl-terminal Random Peptide Library Displayed on λ Phage*—We have assembled a new type of peptide repertoire in which nonapeptides of random sequence are fused to the carboxyl terminus of the D protein and are

[1] The abbreviations used are: hINAD, human INAD (inactivation no after-potential D); nNOS, neuronal nitric-oxide synthase; PSD, postsynaptic density; GST, glutathione *S*-transferase.

[2] P. Vaccaro, unpublished data.

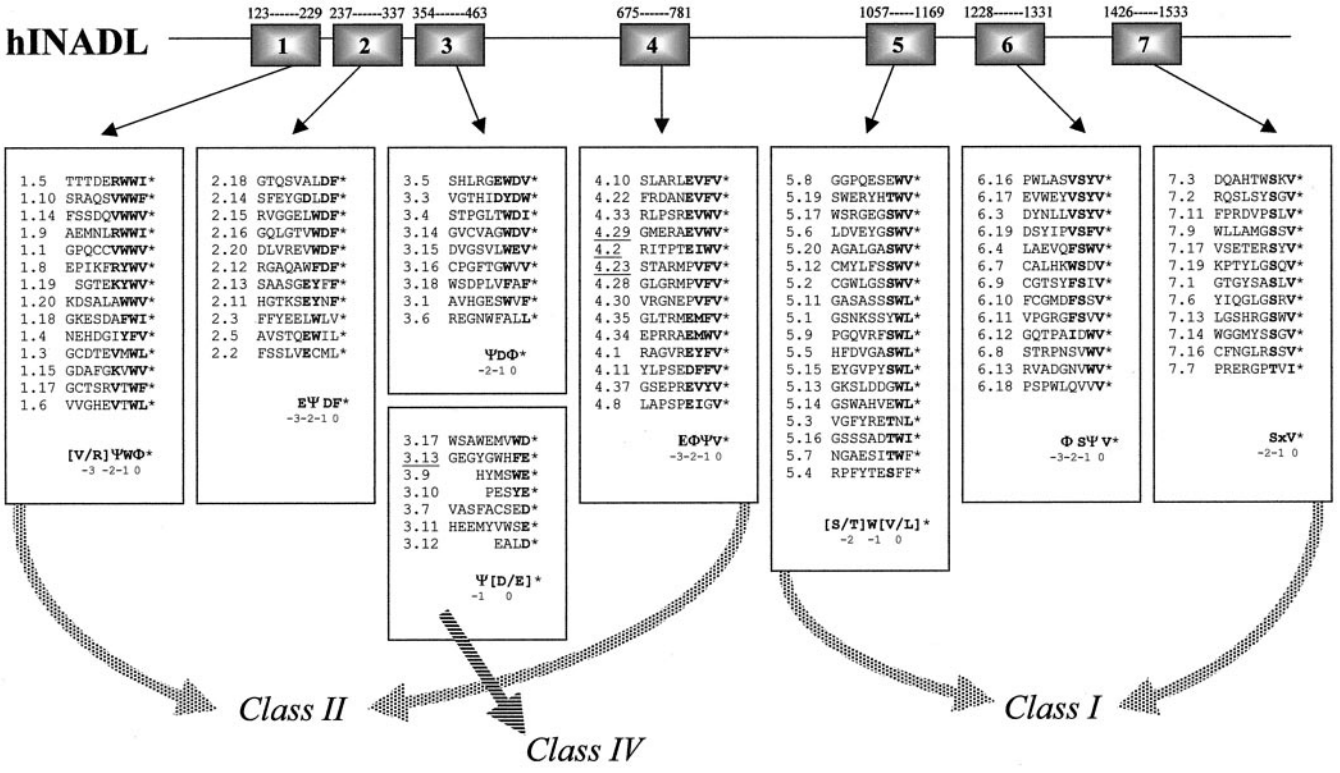


FIG. 1. **Peptides selected by hINADL PDZ domains.** *Top*, schematic representation of hINADL-PDZ domains. The *numbers* above the PDZ domains indicate the first and last residue relative to human INADL sequence (GenBank™ accession number AJ224747) that were included in our GST-PDZ fusion proteins. *Bottom*, lists of PDZ-binding peptides. The *numbers* on the *left* are the names of the phage clones. Clones that were independently isolated more than once are *underlined*. Peptides shorter than nine residues derive from internal stop codons. The single-letter code for amino acids is used; conserved residues are in *bold*; *asterisks* indicate stop codons. Φ and Ψ represent residues with hydrophobic or aromatic side chains respectively. Residues that are conserved in more than 50% of the peptides are represented in the consensus.

efficiently displayed on the surface of the λ phage capsid. To this end we have used a modified vector, λDsplay1 (14) derived from λpRH825 phage constructed by Sternberg and Hoess (36). λDsplay1 drives abundant and stable expression of recombinant D proteins, because one of the loxP sites flanking the D coding sequence and causing genetic instability in the original vector has been deleted. In assembled λ heads, ~95% of the total D protein is chimeric, and the remaining 5% is synthesized by a second wild type gene (14).

The carboxyl-terminal peptide library that we have constructed contains $10^7$ independent clones, each displaying a different nonapeptide. This complexity is sufficient to ensure that all the possible tetrapeptides ($1.6 \times 10^6$) are represented in the library. Since the four carboxyl-terminal residues in the target peptide make the main contacts with the PDZ domain (21–23), this repertoire represents a powerful tool to characterize PDZ peptide recognition specificity. The heterogeneity of the displayed peptides was verified by sequencing the 3′ ends of the D gene in randomly isolated phage clones. A minority of displayed peptides, whose degenerate sequence contains internal stop codons, were shorter than nine residues. To test the effectiveness of the approach, we performed a pilot panning experiment using as bait a PDZ domain whose recognition specificity has already been determined. We overexpressed the third PDZ domain of PSD-95 protein (37) as fusion to GST, and we used it to select ligands from the λ displayed carboxyl-terminal repertoire. All selected peptides matched the carboxyl-terminal sequence of the natural partners (xT/SxV) (6, 29, 38).

*Selection of INADL PDZ Binding Phages*—To identify the preferred ligands of each of the seven PDZ domains of the hINADL protein (12), we constructed a panel of GST fusion proteins, each expressing a different PDZ domain. Domain borders, determined on the basis of the Pfam v5.5 (39) sequence alignment, are indicated in Fig. 1, *top*.

Purified fusion proteins bound to glutathione-Sepharose were used to pan the λ-displayed carboxyl-terminal library. Three selection cycles were sufficient to enrich the number of binding clones of at least 2 orders of magnitude. Phages sorted by panning experiments were further tested by solid phase immunoassay. The selected clones were subjected to DNA sequencing to deduce the amino acidic sequence of the exposed peptides; the sequences were aligned at the carboxyl terminus, and a consensus motif representing the ligands of each domain was derived (Fig. 1). In agreement with previous observations, conserved residues (in *bold*) were only found in the three/four positions preceding the carboxyl terminus (4). Ligand peptides that share a carboxyl-terminal motif containing Ser or Thr at $P^{-2}$, were defined as class I ligands, whereas class II ligands have hydrophobic or aromatic residues at that position (4). According to this criterion INADL-PDZ domains 1, 2, 3, and 4 were found to bind preferentially to class II, whereas PDZ domains 5, 6, and 7 bound to class I ligands.

None of the INADL-PDZ domains showed a preference for class III peptides, characterized by acidic residues in $P^{-2}$ (6). PDZ5 and PDZ6, however, besides the preferred Ser/Thr, also tolerate some acidic or hydrophobic residues at $P^{-2}$.

PDZ3 domain was assigned to a new specificity class, which we designated as class IV, because it was never described before. PDZ3 displays a preference for acidic residues in position $P^0$ in a subgroup of its ligands (the other subgroup conforming to class II). Peptides belonging to either class were

| clone | peptide C-terminus | PDZ 1 | PDZ 2 | PDZ 3 | PDZ 4 | PDZ 5 | PDZ 6 | PDZ 7 | GST |
|---|---|---|---|---|---|---|---|---|---|
| 1-5 | RWWI* | **0.38** | <0.1 | <0.1 | <0.1 | <0.1 | <0.1 | <0.1 | <0.1 |
| 1-14 | VWWV* | **0.50** | **0.40** | **0.35** | <0.1 | **0.20** | **0.30** | <0.1 | <0.1 |
| 2-16 | VWDF* | <0.1 | **0.23** | **0.30** | <0.1 | <0.1 | <0.1 | <0.1 | <0.1 |
| 2-13 | EYFF* | <0.1 | **0.26** | <0.1 | <0.1 | <0.1 | <0.1 | <0.1 | <0.1 |
| 3-16 | GWVV* | <0.1 | <0.1 | **0.52** | <0.1 | <0.1 | <0.1 | <0.1 | <0.1 |
| 3-17 | MVWD* | <0.1 | <0.1 | **0.55** | <0.1 | <0.1 | <0.1 | <0.1 | <0.1 |
| 4-22 | EVFV* | <0.1 | **0.50** | <0.1 | **0.35** | **0.20** | <0.1 | <0.1 | <0.1 |
| 4-23 | PVFV* | <0.1 | <0.1 | <0.1 | **0.60** | <0.1 | <0.1 | <0.1 | <0.1 |
| 5-14 | VEWL* | <0.1 | <0.1 | <0.1 | <0.1 | **0.30** | <0.1 | <0.1 | <0.1 |
| 5-12 | SSWV* | <0.1 | <0.1 | **0.40** | <0.1 | **0.30** | <0.1 | **0.38** | <0.1 |
| 6-4 | FSWV* | <0.1 | <0.1 | <0.1 | <0.1 | **0.30** | **0.25** | **0.25** | <0.1 |
| 6-19 | VSFV* | <0.1 | <0.1 | <0.1 | <0.1 | <0.1 | **0.36** | **0.35** | <0.1 |
| 7-3 | WSKV* | <0.1 | <0.1 | <0.1 | <0.1 | <0.1 | **0.20** | **0.38** | <0.1 |
| 7-7 | PTVI* | <0.1 | <0.1 | <0.1 | <0.1 | <0.1 | <0.1 | **0.38** | <0.1 |

FIG. 2. **Cross-reactivity of PDZ domains.** Two phage clones that display peptides representative of those selected by panning with each of the seven INADL PDZ domains were challenged by solid phase immunoassay with the seven GST-INADL-PDZ domains, immobilized on a multi-well plate. Only the four carboxyl-terminal residues of the displayed peptides are reported in the first column together with the clone number. GST protein was used as control. The values ($A_{405-620\ nm}$) are the average of three independent experiments.

found to bind to the PDZ3 domain with comparable affinity, as judged by solid phase immunoassay (Fig. 2: peptides 3.16 and 3.17). In this respect PDZ3 is unique among the PDZ domains characterized so far, since most members of this domain family prefer hydrophobic residues at the $P^0$ position.

Close inspection of the peptide sequences aligned in Fig. 1 indicates that, aside from the simplified distinction into classes, the seven domains display unique preferences. Peptides that bind to PDZ1 often have basic residues such as Arg or Lys at position $P^{-3}$, (consensus [V/R]ΨWΦ*) (Ψ stands for aromatic, and Φ stands for hydrophobic residue). PDZ2 prefers Phe as the carboxyl-terminal residue and often selects acidic residues at position $P^{-1}$ or $P^{-3}$ (consensus EΨDF*). The peptides selected by PDZ3, by contrast, can be divided into two families; a subset of peptides conforms to type II with preference for Asp at $P^{-1}$ (consensus ΨDΦ*), and the remaining peptides define the novel class IV (consensus Ψ[D/E]*). PDZ4 prefers aromatic, hydrophobic, and acidic residues at positions $P^{-1}$, $P^{-2}$, and $P^{-3}$, respectively (consensus EΦΨV*). PDZ5 has a strong preference for Trp at $P^{-1}$ (consensus [S/T]W[VL]*) and can bind peptides with Glu at $P^{-2}$. The PDZ6 binding consensus is similar to the one of PDZ5 but shows a higher variability both at $P^{-1}$ and $P^{-2}$. At $P^{-3}$ hydrophobic residues are preferred (consensus ΦSΨV*). Finally, PDZ7 is a canonical class I domain that has a marked preference for Ser at $P^{-2}$ and Val at $P_0$ and very little selectivity, if any, at $P^{-1}$ and $P^{-3}$ (consensus [S] × [V]*).

*Cross-reactivity of PDZ Domains*—To test the cross-reactivity of the different PDZ domains, we performed a solid phase immunoassay where two representative phage clones for each domain were challenged with all the remaining INADL-PDZ domains immobilized on a multi-well plate (Fig. 2). The analysis revealed that some peptides have a high specificity and only bind to one domain; others were found to be more promiscuous and reacted also with domains different from the one that originally selected them in the panning experiment. In most cases, cross-reacting domains, as defined by this test, belong to the same domain class. As expected, PDZ7 displayed the lowest specificity, accepting any peptide containing Ser or Thr at position $P^{-2}$. By contrast, PDZ1 and PDZ4 are characterized by the highest selectivity and do not bind to any of the peptides selected by the other domains.

*Site-directed Mutagenesis of Contact Positions and Homology Modeling*—To contribute to the characterization of the molecular basis of the binding specificity mediated by PDZ domains, we generated site-directed mutations in the PDZ7 domain, with the aim of altering its ligand preference and converting it into a domain with class II binding specificity.

The contact matrix in Fig. 3*a* was derived from the analysis of the three-dimensional structures of PDZ domains crystallized with their targets (21, 22, 23). The four rows represent the four carboxyl-terminal positions of a ligand peptide, whereas the 23 columns represent the PDZ residues that contact the target peptide in at least one of the complexes of known structure. Two residues are defined as being in contact when, in any of the three complexes of known crystallographic structure, the shortest distance between their atoms is less than the sum of their van der Waals radii ($r$) + 3 Å (Fig. 3, *gray cells*). When the distance is shorter than $r$ + 0.6 Å, the cell at the intersect is shown in *black*. To identify residues that may be involved in target recognition in hINADL-PDZ domains, we aligned their primary sequences with those of the three crystallized domains. Several residues in the contact positions (in *bold*) are conserved (Fig. 3*b*). The first residue of the helix αB, corresponding to position 16 in the contact matrix, was found to influence the preference for specific residues at $P^{-2}$ in the ligand peptide (4, 6, 40). His at that location correlates with preference for Ser/$Thr^{-2}$ (class I), whereas PDZ domains containing a hydrophobic residue preferentially bind to class II ligands (4, 23, 41). The results that we have obtained with the PDZ domains of hINADL are only partially in accord with these observations. The three class I-PDZ domains of hINADL have His at contact position 16 (*shadowed* in Fig. 3), but among the four class II-PDZ domains, PDZ1 has His and only PDZ4 has a hydrophobic amino acid (Leu) at position 16.

To convert the class specificity of PDZ7, we changed by site-directed mutagenesis, the di-peptide $H^{16}E^{17}$ in PDZ7 (class I) into $L^{16}A^{17}$, as in the corresponding helix of PDZ4 (class II). The ligand preferences of the mutated domain PDZ7LA were analyzed by panning the λ-displayed carboxyl-terminal library (Fig. 4). Phages selected by PDZ7LA do not bind to wild type PDZ7 in solid phase immunoassay. On the other hand, we did not observe a clear shift from class I to class II specificity but rather a decrease in selectivity of the mutant domain, since no preference for a specific residue at $P^{-2}$ was detected. Both class II and class I ligands were represented among the selected peptides. Thus the dipeptide $L^{16}A^{17}$ was not sufficient to graft onto PDZ7 the striking preference for a hydrophobic residue at $P^{-2}$, as observed for PDZ4.

To rationalize this result, we used homology modeling to build and compare the three-dimensional models of mutant PDZ7LA domains in complex with peptide LA11 carboxyl-terminal residues (RVSV*) and wild-type PDZ7 in complex with one of its target peptides, 7.16 (RSSV*). When the mutant and the wild type models are compared, the most prominent difference is the larger cavity observed in the mutant binding site (Fig. 5). We used SURFNET, a procedure for visualizing molecular surfaces, cavities, and intermolecular interactions (19) to measure the volume of the two clefts; the difference between the mutant and the wild type cavities (shown in *magenta* in Fig. 5) is about 60 $Å^3$. This structural feature is consistent with the experimental observation that the binding pocket has become less selective and tolerates residues with large side chains at $P^{-2}$.

PDZ7 accepts any residue at position $P^{-1}$, where, in contrast, PDZ4 prefers aromatic residues. Several contact positions might influence this preference. Residues at βB2 (position 7 in the contact matrix in Fig. 3) and βC5 (position 13) have been suggested to be the main determinants of side chain preference at $P^{-1}$ (38). Since PDZ7 and PDZ4 have the same residue (Ser) at position 7, we decided to exchange residues of the βC strand that in the matrix are predicted to contact the ligand at $P^{-1}$

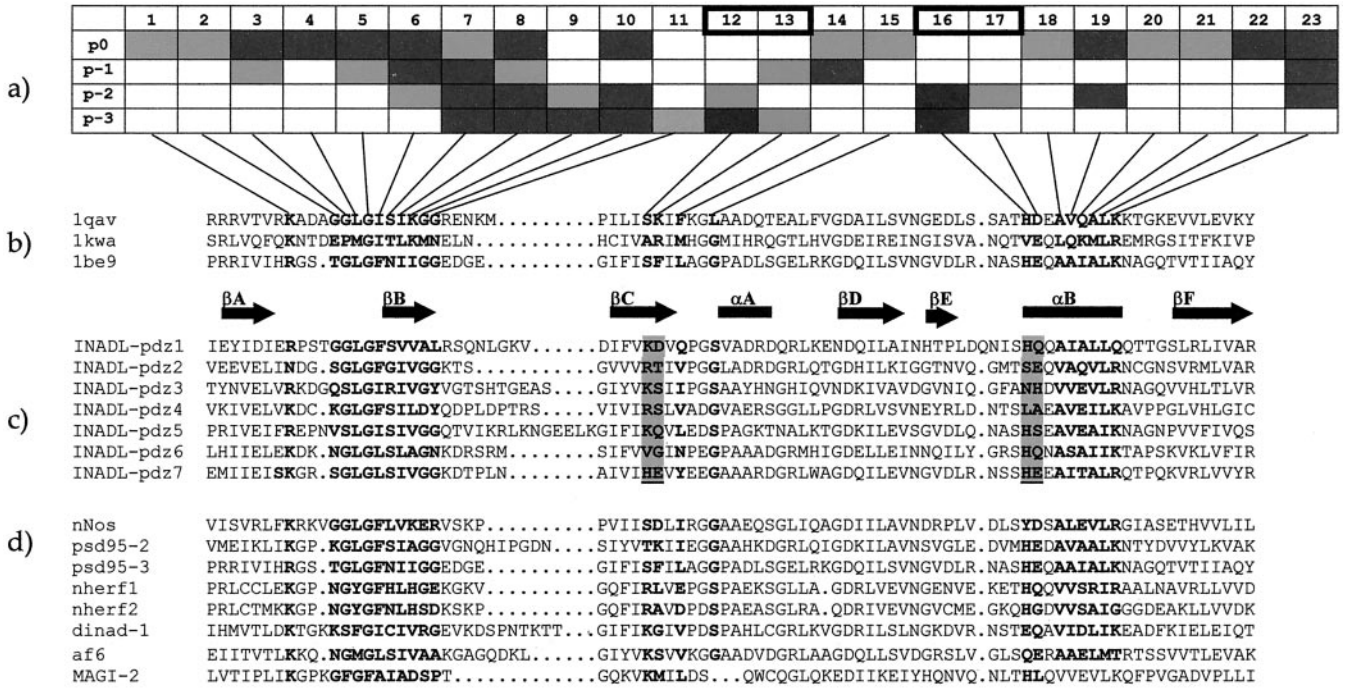


FIG. 3. **PDZ-specific contact matrix.** A contact point matrix was derived from the three-dimensional structures of PDZ domains crystallized with their targets (see "Experimental Procedures"). The *rows* represent the four carboxyl-terminal positions of a ligand peptide, and the *columns* represent the 23 positions of the multiple alignment of PDZ sequences that contact the target peptide. The *lines* leading from the columns extend to residues in the PDZ sequence that contact one or more residues in the target. Cells at the intersect are *shaded* according to the distance between the interacting atoms; *gray* or *black colors* correspond to distances shorter than the sum of the van der Waals radii ($r$) + 3 Å or $r$ + 0.6 Å, respectively. *b*, multiple alignment of the sequences of PDZ domains whose structure in complex with a target peptide has been solved. The PDZ residues in contact with residues of the peptide are shown in *bold*. *c*, multiple alignment of the hINADL-PDZ domain sequences. Positions 12–13 and 16–17, which were altered by site-directed mutagenesis in this work, are *shaded*. *d*, multiple alignment of the sequences of the other PDZ domains, whose peptide ligands were inserted in the SPOT data base.

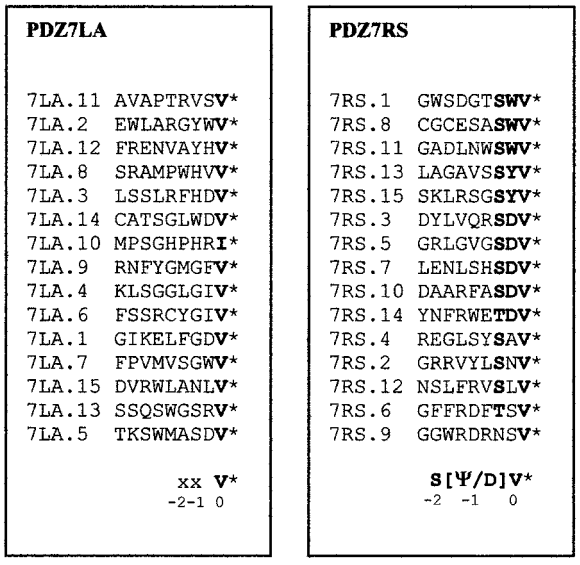


FIG. 4. **Peptides selected by PDZ7 mutant domains.** *Numbers* and *symbols* are defined as in the legend of Fig. 1.

and $P^{-3}$. Amino acids $H^{12}E^{13}$ of PDZ7 were substituted with $R^{12}S^{13}$ as in PDZ4. The ligand preference of mutant PDZ7RS was determined by panning phage-displayed peptide repertoires. The consensus sequence (S[Ψ/D]V*), derived from the selected peptides (Fig. 4), identifies an acquired preference for peptides carrying either an aromatic residue or an Asp at $P^{-1}$. Whereas the aromatic residue at $P^{-1}$ is consistent with the PDZ4 consensus, the preference for Asp was not anticipated. On the other hand, we have observed that the two domains displaying specificity for acidic residues at $P^{-1}$, PDZ2 and PDZ3, have similar residues at the positions that we have mutated, $R^{12}T^{13}$) and ($K^{12}S^{13}$), respectively.

All peptides selected by PDZ7RS are class I ligands; they also bind to wild type PDZ7 when tested by solid immunoassay (data not shown). We compared the homology models of PDZ7 and PDZ7RS domains, in complex with the carboxyl-terminal residues of peptide RS14 (ETDV*) (Fig. 6). In the PDZ7RS·RS14 model complex, the residue at position 12 forms an additional hydrogen bond with the side chain of the residue at position $P^{-1}$ of the ligand. After energy minimization, the lowest energy level for this complex was reached with the Asp ($P^{-1}$) side chain pointing toward the side chain of the mutated $Arg^{12}$. In contrast, the Asp ($P^{-1}$) side chain of the peptide is solvent-exposed in the wild-type/peptide model.

In principle the identity of the side chains at position 12 and 13 should also influence the amino acid preference at $P^{-3}$, where PDZ4, different from PDZ7, shows a preference for acidic side chains. However, exchange of the residues at positions 12 and 13 was not sufficient to transfer this specificity from PDZ4 to PDZ7, since only one of the selected peptides (RS14) has a Glu at $P^{-3}$. In both the three-dimensional models shown in Fig. 6, the side chain of Glu at $P^{-3}$ of the RS14 peptide points toward Arg or His at position 12.

*Application of the SPOT Algorithm to PDZ Domains*—By changing some residues in the PDZ peptide binding pocket, we have been able to modulate the recognition specificity of this domain. However, different from previous reports, our experiments have not revealed simple rules that permit the inference the preferred ligand of PDZ domains. This suggests that several contacts may influence the preferred amino acid

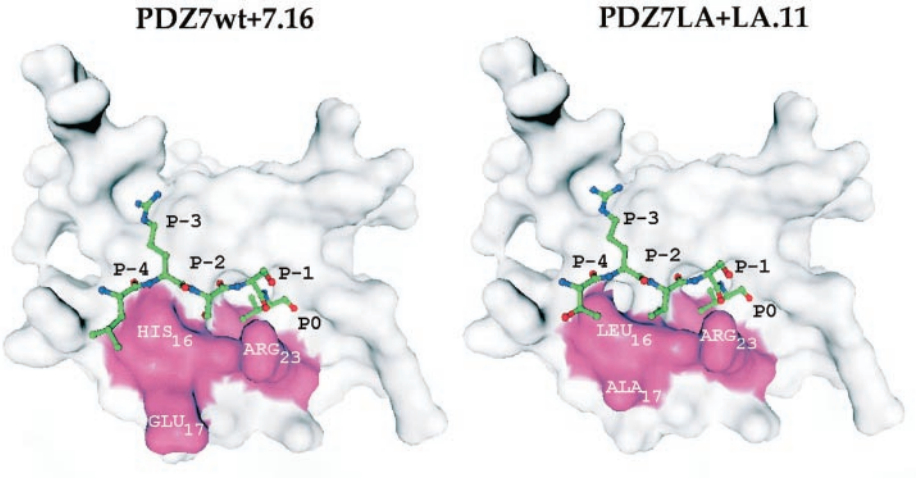


FIG. 5. **Model complex of PDZ7 and PDZ7LA domains with their peptide ligands.** Surface representation of domain-ligand complexes obtained with the WebLab WieverLite 3.20 software by Molecular Simulations Inc. (*www.msi.com/life/products/weblab/index.html*). Residues that form the binding pocket that hosts the side chain at $P^{-2}$ in the ligand peptide are indicated with *white letters* and *purple*. In the wild type PDZ7 the shortest distance between His-16 and Arg-23 is 7.85 Å; in the LA mutant the distance between Leu-16 and Arg-23 is 9.09 Å.

at the different ligand positions in a way that is often difficult to predict. To approach a similar problem related to recognition specificity mediated by SH3 domains, the algorithm SPOT (Specificity Prediction of Target) was recently developed (20). This is based on a statistical method that, by taking into account the frequency with which residue *X* in the domain binding surface faces residue *Y* in a collection of ligand peptides at any of the contact positions, permits the evaluation of the likelihood that any SH3 domain binds to any peptide.

The applicability of the approach depends on the availability of crystal structures of at least one domain-peptide complex to identify the contact positions and of a collection, as large as possible, of experimentally determined ligands for a variety of domains of the same family. Furthermore, the domain family and the ligand peptides should be sufficiently homogeneous to permit their confident alignment in the binding region, to allow a correct identification of the residues in the defined contacting positions. The sequence identity between the PDZ domains (shown in Fig. 3*b*) and the INADL PDZ domains (Fig. 3*c*) allows a fairly reliable alignment of their sequences, and the ligand peptides can be unambiguously aligned since they all bind the PDZ domains through their carboxyl-terminal end. The results of the phage display screening described above substantially enrich the collection of specific ligands of PDZ domains so far available and may permit the extension of the SPOT algorithm to the PDZ domain.

The matrix shown in Fig. 3 defines the PDZ/peptide contacts. Each of these contact positions is associated to a $20 \times 20$ matrix that contains the frequencies of occurrence of the residues observed in those positions in PDZ domains and peptides able to form a stable complex. This data base was constructed using available experimental data deriving from the screenings of combinatorial repertoires with PDZ domains or from reports where multiple ligands for the same PDZ domain were described (see "Experimental Procedures").

SPOT permits the ranking of a collection of peptides according to their propensity to bind a specific domain or to infer the sequence of a consensus ligand by comparing the amino acid sequence of the peptides that obtain the highest scores. This can in turn be matched to the experimentally determined consensus. When this procedure is applied to the 7 PDZ domains of INADL, in all cases the SPOT consensus compares well with that experimentally determined.

We then questioned whether the information provided to the algorithm was sufficient to infer the interaction of ligands that were not included in the interaction data base. For this purpose we chose to investigate the performance of SPOT when tested

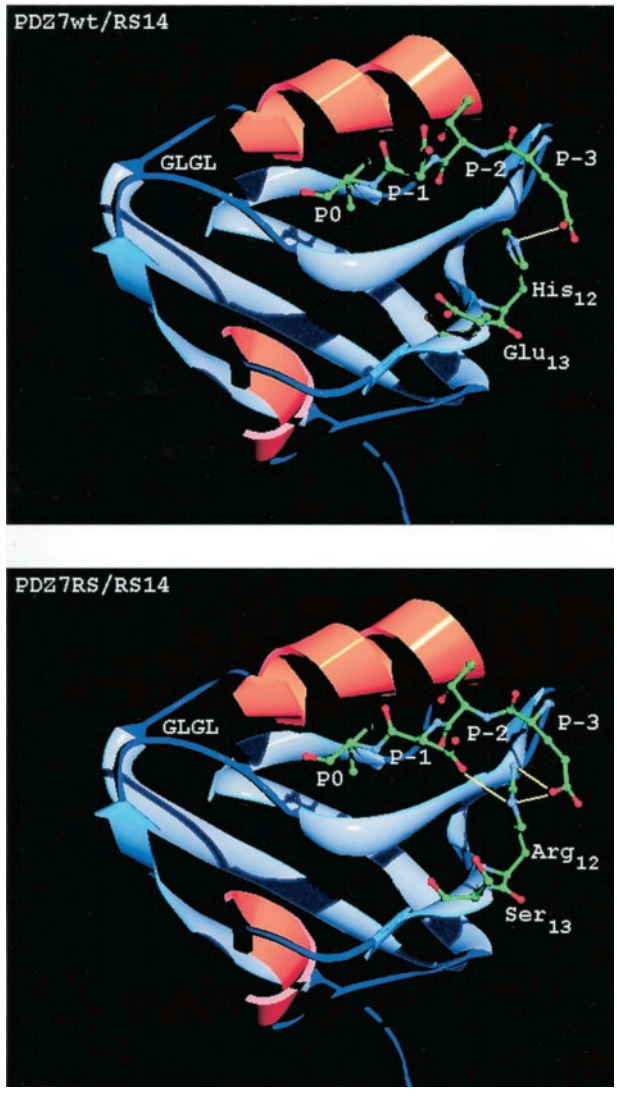


FIG. 6. **Model complexes of PDZ7 and PDZ7RS domains with the peptide ligand RS14 (ETDV*).** Ribbon diagram of the domain/ligand complexes obtained with the Swiss-PDBWiever software v3.7b2 and with the POV-Ray™ software (www.povray.org) (48). The side chains of the residues that were mutated, and the peptide ligands are shown. The hydrogen bonds (*yellow sticks*) formed by the residues at position 12 in the models are *highlighted*. According to the model derived from the structure of PSD95-3 complexed with its ligand (23), the residue at position 12 in PDZ7 wild type forms one hydrogen bond with the side chain at $P^{-3}$ in the peptide. In contrast, the Arg at position 12 of PDZ7RS forms a second hydrogen bond with position $P^{-1}$.

TABLE I
*Application of the SPOT algorithm to the MUPP1 PDZ domains and their ligands*

PDZ domains are numbered from 1 to 13 and ordered according to the SPOT score. The experimentally defined binding domains are indicated in bold. Binding of NG2 to MUPP1-PDZ1 and of 5-HT2 receptors to MUPP-1 PDZ10 were determined by two-hybrid analysis and pull-down and immunoprecipitation assays (43, 44). Binding of E4 orf1 to MUPP1 (9BP-1) was identified by screening a λgt11 cDNA expression library (42); pull-down and immunoprecipitation assays allowed definition of PDZ7 and PDZ10 as preferential binding regions (45).

| Experimentally determined ligand | Ranking of MUPP1 PDZ domains (without INADL data) | Ranking of MUPP1 PDZ domains (with INADL data) |
|---|---|---|
| NG2 (QYWV*) | 9 10 **1** 11 7 4 5 6 3 13 2 12 8 | **1** 9 4 6 11 7 3 13 10 12 2 5 8 |
| 5-HT2C (VSCV*) | 5 11 7 **10** 9 6 1 13 12 3 4 2 8 | **10** 8 13 11 7 3 4 9 6 1 12 2 5 |
| 5-HT2B (VSYV*) | 5 **10** 11 6 7 3 9 1 13 4 2 12 8 | **10** 8 3 11 13 7 4 6 9 1 2 12 5 |
| 5-HT2A (ISSV*) | 5 11 **10** 1 7 9 13 6 4 2 3 12 8 | **10** 11 13 7 8 4 3 9 1 5 6 12 2 |
| E4 orf1 (ATLV*) | 5 1 11 **10** 13 7 4 2 3 6 9 12 8 | 13 11 **10** 2 4 7 6 3 9 1 5 12 8 |

on MUPP1, a protein of the multi PDZ family containing the highest number of PDZ domains. MUPP1 was identified in three independent laboratories on the basis of its ability to bind to the carboxyl terminus of the serotonin (5-HT2C) receptor (13), of the 9ORF1 viral transforming protein (42), and of NG2 proteoglycan (43). Although the MUPP1 domains that are responsible for target recognition have been experimentally determined, the binding specificity of the different MUPP1 PDZ domains was never investigated in detail. We have used the SPOT algorithm to establish which of the 13 PDZ domains is most likely to be responsible for binding to the carboxyl terminus of the proteins that were found to form a complex with MUPP1. The carboxyl-terminal residues of each MUPP1 protein ligand were ranked by SPOT against the 13 PDZ domains (Table I). The size of the data base clearly influences the performance of the algorithm, since the addition of the INADL ligand peptides significantly improved the prediction results. The SPOT inferred and the experimentally determined binding domains compared rather well; PDZ1, the main binder for NG2 proteoglycan (43), is ranked first by SPOT. PDZ10 obtains the highest score when tested with 5-HT2A, -2B, -2C receptors carboxyl-terminal peptides, in agreement with the results of two-hybrid binding assays (44). Finally, PDZ13 and PDZ11 are predicted to be the best ligands of the 9ORF1 peptide, with PDZ10 ranking third, whereas experimental data indicate that PDZ10 and PDZ7 are the receptors of the carboxyl terminus of 9ORF1 (45). The predictive reliability of the method will increase with the enrichment of the PDZ-specific matrix with interaction data derived from more comprehensive lists of peptide ligands. In this respect, the approach that we have developed, based on the screening of λ-displayed carboxyl-terminal peptide libraries, is likely to facilitate the rapid accumulation of new binding information.

## DISCUSSION

PDZ domains are frequently found in proteins associated with the cellular membrane, where they coordinate the assembly of trans-membrane and cytosolic components into multiprotein complexes. Multiple PDZ domains, often in association with other modules such as SH3, guanylate kinase, etc. may be found in a single polypeptide, suggesting that these modules have been utilized in evolution to assemble protein adapters that work as scaffolds to cluster and regulate the activity of various proteins (1, 4, 5). Some PDZ domains promote colocalization of target proteins to different sub-cellular compartments (3). Schneider *et al.* (46) elegantly show that it is possible to modulate this activity *in vivo* by exploiting artificial PDZ domains (46). Understanding the principles whereby distinct binding domains recognize their substrates provides the rationale to infer the recognition specificity of a domain from its primary sequence. The rules underlying the recognition specificity of PDZ domains are only partially understood (3, 46). Different from other protein binding modules, PDZ domains show a preference for binding to the free carboxyl terminus of target proteins. In some cases they may also dimerize with other PDZ-containing proteins by binding to an internal region folded in a β-hairpin finger (21, 40). This structure mimics a free carboxyl-terminal peptide, which can be fitted into the binding pocket of the receptor domain (21). All PDZ domains whose three-dimensional structure have been solved contain a core of five or six β-sheets (βA-βF) and two α-helices (αA and αB). The ligand fits into a hydrophobic pocket created by the α-helix (αB), the second β-strand (βB), and the conserved GLGF loop that connects the βA and βB strands.

Depending on the consensus sequence of preferred ligands, PDZ domains have been grouped into classes. Often domains that belong to the same class share conserved residues in crucial contact positions of the binding pocket (4). Class I PDZ domains bind to peptides containing the (S/T)*X*V motif and have a conserved His as first residue of α-helix B (αB1). Class II PDZ domains favor a Φ/Ψ*X*Φ motif and have a hydrophobic residue at αB1 (4, 22). Class III is represented by Mint PDZ that binds to peptides with (E/D)*X*W(C/S) consensus sequence (47) and by nNOS PDZ, which has a preference for ligands with negatively charged amino acids at $P^{-2}$ (6, 40). Stricker *et al.* (6) show that substitutions of αB1-αB2 residues change the binding specificity of nNOS to class I type (6). Finally, positions $P^{-3}$ and $P^{-1}$, previously considered irrelevant for binding because they are solvent-exposed in the PSD95-3/peptide structure (23), turned out to be important in determining the binding of other domains (8, 38).

These simplified rules are not always sufficient in explaining the binding preferences of distinct PDZ domains. For instance, INADL PDZ1, which has a His at αB1 (position 16 in the matrix in Fig. 3), according to these rules should be classified as class I domain. On the other hand, PDZ1 and PDZ4 that have a Ser at βB2 (position 7) would be predicted to bind to peptides containing Asp at $P^{-1}$ (38).

We defined the binding preference of the seven PDZ domains of INADL by screening a repertoire of random peptides displayed at high density on the capsid of bacteriophage λ. The high display density guarantees that because of avidity effects, relatively low affinity ligands (10 μM) are not at a disadvantage in the binding step. This is particularly important since sometimes the physiologically relevant PDZ ligands are not the ones that bind with the highest affinity (8). Therefore, it was important to identify most of the residues that are accepted at each peptide position by each PDZ domain of INADL irrespective of the relative affinity of the single peptides.

A different consensus binding sequence was defined for each INADL PDZ domain. In some cases the result was in contrast with the predictions based upon the rules cited above. The seven PDZ domains are arranged into two blocks of class II (PDZ1–4) and class I (PDZ5–7) domains. The question of

whether this ordered topographical distribution has any physiological relevance is likely to be answered by the identification of the natural INADL-interacting proteins. At the moment, INADL is an "orphan" adapter protein, whose natural targets are unknown.

The PDZ3 domain was found to bind to two distinct classes of peptides. One family is a typical class II, whereas the second family is defined by a Asp or Glu as the carboxyl-terminal residue. With the exception of Mint-1 (class III), which binds to peptides ending with Cys or Ser, all the other known PDZ domains bind to peptides characterized by hydrophobic or aromatic terminal residues. Therefore, INADL-PDZ3 represents a novel class (class IV) of PDZ domains.

In principle the peptide binding consensus can be used as patterns to search protein data bases for proteins that contain carboxyl-terminal residues that match the consensus. This approach was shown to be successful in the case of several SH3 domains (2) and of few PDZ domains (5). The consensus that characterize the ligands of PDZ domains, however, are poorly selective, and these pattern search experiments yield far too many candidate partners to be useful as a hint to guide more complex biological experiments. For instance, an attempt to scan the Trembl/Swiss-Prot data base with the class IV consensus for potential PDZ3-interacting proteins yielded multiple matches, among these, several ion channels, tyrosine kinase substrates, and viral proteins, whose physiological binding relevance should be experimentally tested.

Each hINADL-PDZ domain, with the exception of PDZ7, showed specific preferences not only for residues at position $P^{-2}$ (defining the class) but also for positions $P^{-3}$ and $P^{-1}$. These further differences in the binding specificity might enhance the combinatorial possibilities for assembling different proteins into a complex.

Mutagenesis experiments aimed at altering the preference for one of the four ligand positions are very informative and help in the design of artificial PDZ domains with desired properties (46) or in the prediction of putative ligand for a given PDZ. Substitution of the second residue of the $\beta$B strand of PSD-95 PDZ3 from Gln to Ser, changed its preference for ligands carrying Asp or Glu at $P^{-1}$ (38), whereas changing the dipeptide $Y^{16}D^{17}$ of nNOS PDZ into $H^{16}E^{17}$ (the first two residues of $\alpha$B helix) altered its preference for the residue at $P^{-2}$ (6). In this paper we have shown that substitution of amino acids $H^{12}E^{13}$ of PDZ7 with $R^{12}S^{13}$ (as in PDZ4) induced an acquired preference for peptides carrying either an aromatic residue or an aspartate at $P^{-1}$. On the other hand, substitution of the dipeptide $H^{16}E^{17}$ of hINADL-PDZ7 into $L^{16}A^{17}$ was not sufficient to convert the class I specificity of PDZ7 into class II, as one would have expected from previous analyses (6).

All together the experiments described in this manuscript substantially enrich the information on PDZ recognition specificity so far available and permit the extension of the applications of the SPOT algorithm to the PDZ domain family. Anyway, the possibility to compute a complete PDZ-specific matrix depends upon the availability of interaction data coming from as many as possible different families of PDZ domains. Because the procedure is based on the assumption that the interaction between two proteins can be described in a first approximation as the sum of independent interactions between their contacting residues (see "Experimental Procedures"), a reliable prediction can be obtained by the SPOT procedure only if the matrix contains data about PDZ domains sharing at least some sequence identity with the query PDZ domains. The results shown in Table I demonstrate that the INADL interaction data obtained in the experiments described in this work substantially helped in the construction of a more complete PDZ-specific matrix. Specifically, the new interaction data of the INADL PDZ domains added information about the preferred interactions of residues in the binding pocket of the MUPP1-PDZ domains, which were previously missing from the PDZ-specific matrix. The good correlation between experimental results (43, 44, 45) and SPOT predictions confirmed the validity of the approach. However further experimental results about the binding specificity of more PDZ domains need to be added to the PDZ-specific matrix before inferring with confidence the specificity of any member of the PDZ family.

*Acknowledgments*—We are grateful to V. Flockerzi (Universität des Saarlandes, Homburg) for the human INADL cDNA clone.

REFERENCES

1. Pawson, T., and Scott, J. D. (1997) *Science* **278,** 2075–2080
2. Kay, B. K., Kasanov, J., Knight, S., and Kurakin, A. (2000) *FEBS Lett.* **480,** 55–62
3. Fanning, A. S., and Anderson J. M. (1999) *Cur. Opin. Cell Biol.* **11,** 432–439
4. Songyang, Z., Fanning, A. S., Fu, C., Xu, J., Marfatia, S. M., Chishti, A. H., Crompton, A., Chan, A. C., Anderson, J. M., and Cantley, L. C. (1997) *Science* **275,** 73–77
5. Schultz, J., Hoffmuller, U., Krause, G., Ashurst, J., Macias, M. J., Schmieder, P., Schneider-Mergener, J., and Oschkinat, H. (1998) *Nat. Struct. Biol.* **5,** 19–24
6. Stricker, N. L., Christopherson, K. S., Yi, B. A., Schatz, P. J., Raab, R. W., Dawes, G., Bassett, D. E., Jr., Bredt, D. S., and Li, M. (1997) *Nat. Biotechnol.* **15,** 336–342
7. Gee, S. H., Sekely, S. A., Lombardo, C., Kurakin, A., Froehner, S. C., and Kay, B. K. (1998) *J. Biol. Chem.* **273,** 21980–21987
8. Fuh, G., Pisabarro, M. T., Li, Y., Quan, C., Lasky, L. A., and Sidhu, S. S. (2000) *J. Biol. Chem.* **275,** 21486–21491
9. Wilson, D., and Findlay, R. (1998) *Can. J. Microbiol.* **44,** 313–329
10. Banner, D. W., Nave, C., and Marvin, D. A. (1981) *Nature* **289,** 814–816
11. Yang, F., Forrer, P., Dauter, Z., Conway, J. F., Cheng, N., Cerritelli, M. E., Steven, A. C., Pluckthun, A., and Wlodawer, A. (2000) *Nat. Struct. Biol.* **7,** 230–237
12. Philipp, S., and Flockerzi, V. (1997) *FEBS Lett.* **413,** 243–248
13. Ullmer, C., Schmuck, K., Figge, A., and Lubbert, H. (1998) *FEBS Lett.* **424,** 63–68
14. Castagnoli, L., Zucconi A., Quondam, M., Rossi, M., Vaccaro, P., Panni, S., Paoluzi, S., Santonico, E., Dente, L., and Cesareni, G. (2001) *Combinatorial Chem. and High Throughput Screening,* **4,** 121–133
15. Zucconi, A., Dente, L., Santonico, E., Castagnoli, L., and Cesareni, G. (2001) *J. Mol. Biol.* **307,** 1329–1339
16. Santi, E., Capone, S., Mennuni, C., Lahm, A., Tramontano, A., Luzzago, A., and Nicosia, A. (2000) *J. Mol. Biol.* **296,** 497–508
17. Bernstein, F. C., Koetzle, T. F., Williams, G. J. B., Meyer, E. F., Brice, M. D., Rodgers, J. R., Kennard, O., Shimanouchi, T., and Tasumi, M. (1977) *J. Mol. Biol.* **112,** 535–542
18. Dayringer, H. E., Tramontano, A., Sprang, S. R., and Fletterick, R. J. (1986) *J. Mol. Graph.* **4,** 82–87
19. Laskowski, R. A. (1995) *J. Mol. Graph.* **13,** 323–330
20. Brannetti, B., Via A., Cestra, G., Cesareni, G., and Helmer-Citterich, M. (2000) *J. Mol. Biol.* **298,** 313–328
21. Hillier, B. J., Christopherson, K. S., Prehoda, K. E., Bredt, D. S., and Lim, W. A. (1999) *Science* **284,** 812–815
22. Daniels, D. L., Cohen, A. R., Anderson, J. M., and Brunger, A. T. (1998) *Nat. Struct. Biol.* **5,** 317–325
23. Doyle, D. A., Lee, A., Lewis, J., Kim, E., Sheng, M., and MacKinnon, R. (1996) *Cell* **85,** 1067–1076
24. Schepens, J., Cuppen, E., Wieringa, B., and Hendriks, W. (1997) *FEBS Lett.* **409,** 53–56
25. Hock, B., Bohme, B., Karn, T., Yamamoto, T., Kaibuchi, K., Holtrich, U., Holland, S., Pawson, T., Rubsamen-Waigmann, H., and Strebhardt, K. (1998) *Proc. Natl. Acad. Sci. U. S. A.* **95,** 9779–9784
26. Buchert, M., Schneider, S., Meskenaite, V., Adams, M. T., Canaani, E., Baechi, T., Moelling, K., and Hovens, C. M. (1999) *J. Cell Biol.* **144,** 361–371
27. Kim, E., Niethammer, M., Rothschild, A., Jan Y. N., and Sheng, M. (1995) *Nature* **378,** 85–88
28. Kornau, H. C., Schenker, L. T., Kennedy, M. B., and Seeburg, P. H. (1995) *Science* **269,** 1737–1740
29. Irie, M., Hata, Y., Takeuchi, M., Ichtchenko, K., Toyoda, A., Hirao, K., Takai, Y., Rosahl, T. W., and Sudhof, T. C. (1997) *Science* **277,** 1511–1515
30. Gee, S. H., Madhavan, R., Levinson, S. R., Caldwell, J. H., Sealock, R., and Froehner, S. C. (1998) *J. Neurosci.* **18,** 128–137
31. Cohen, A. R., Woods, D. F., Marfatia, S. M., Walther, Z., Chishti, A. H., and Anderson, J. M. (1998) *J. Cell Biol.* **142,** 129–138
32. Hsueh, Y., Yang, F., Kharazia, V., Naisbitt, S., Cohen, A. R., Weinberg, R. J., and Sheng, M. (1998) *J. Cell Biol.* **142,** 139–151
33. van Huizen, R., Miller, K., Chen, D. M., Li, Y., Lai, Z. C., Raab, R. W., Stark, W. S., Shortridge, R. D., and Li, M. (1998) *EMBO J.* **17,** 2285–22897
34. Wes, P. D., Xu, X. Z., Li, H. S., Chien, F., Doberstein, S. K., and Montell, C. (1999) *Nat. Neurosci.* **5,** 447–453
35. Wang, S., Raab, R. W., Schatz, P. J., Guggino, W. B., and Li, M. (1998) *FEBS Lett.* **427,** 103–108
36. Sternberg, N., and Hoess, R. H. (1995) *Proc. Natl. Acad. Sci. U. S. A.* **92,** 1609–1613

37. Stathakis, D. G., Hoover, K. B., You, Z., and Bryant, P. J. (1997) *Genomics* **1,** 7–11
38. Niethammer, M., Valtschanoff, J. G., Kapoor, T. M., Allison, D. W., Weinberg, T. M., Craig, A. M., and Sheng, M. (1998) *Neuron* **20,** 693–707
39. Sonnhammer, E. L. L., Eddy, S. R., Birney, E., Bateman, A., and Durbin, R. (1998) *Nucleic Acids Res.* **26,** 320–322
40. Tochio, H., Zhang, Q., Mandal, P., Li, M., and Zhang, M. (1999) *Nat. Struct. Biol.* **6,** 417–421
41. Kornau, H. C., Seeburg, P. H., and Kennedy, M. B. (1997) *Curr. Opin. Neurobiol.* **3,** 368–373
42. Lee, S. S., Weiss, R. S., and Javier, R. T. (1997) *Proc. Natl. Acad. Sci. U. S. A.* **94,** 6670–6675
43. Barritt, D. S., Pearn, M. T., Zisch, A. H., Lee, S. S., Javier, R. T., Pasquale, E. B., and Stallcup, W. B. (2000) *J. Cell. Biochem.* **79,** 213–224
44. Becamel, C., Figge, A., Poliak, S., Dumuis, A., Peles, E., Bockaert, J., Lubbert, H., and Ullmer, C. (2001) *J. Biol. Chem.* **276,** 12974–12982
45. Lee, S., S., Glaunsinger, B., Mantovani, F., Banks, L., and Javier, R., T. (2000) *J. Virol.* **74,** 9680–9693
46. Schneider, S., Buchert, M., Georgiev, O., Catimel, B., Halford, M., Stacker, S. A., Baechi, T., Moelling, K., and Hovens, C. M. (1999) *Nat. Biotechnol.* **17,** 170–175
47. Maximov, A., Sudhof, T. C., and Bezprozvanny, I. (1999) *J. Biol. Chem.* **274,** 24453–24456
48. Guex, N., and Peitsch, M. C. (1997) *Electrophoresis* **18,** 2714–2723

**Distinct Binding Specificity of the Multiple PDZ Domains of INADL, a Human Protein with Homology to INAD from *Drosophila melanogaster***

Paola Vaccaro, Barbara Brannetti, Luisa Montecchi-Palazzi, Stephan Philipp, Manuela Helmer Citterich, Gianni Cesareni and Luciana Dente

*J. Biol. Chem. 2001, 276:42122-42130.*
*doi: 10.1074/jbc.M104208200 originally published online August 16, 2001*

---